



Obrabotka metallov -

Metal Working and Material Science

Journal homepage: http://journals.nstu.ru/obrabotka_metallov



Features of calculating the cutting temperature during high-speed milling of aluminum alloys without the use of cutting fluid

Dmitry Gubin^{1, a}, Anton Kisel'^{2, b, *}

¹ Omsk State Technical University, 11 Prospekt Mira, Omsk, 644050, Russian Federation

² Kaliningrad State Technical University, 1 Sovetsky Prospekt, Kaliningrad, 236022, Russian Federation

^a  <https://orcid.org/0000-0003-1825-1310>,  gubin.89@list.ru; ^b  <https://orcid.org/0000-0002-8014-0550>,  kisel1988@mail.ru

ARTICLE INFO

Article history:

Received: 19 October 2023

Revised: 16 November 2023

Accepted: 22 January 2024

Available online: 15 March 2024

Keywords:

Cutting temperature

High-speed milling

Aluminum alloy

Homologous temperature

Thermal imager

Forecasting

Specific work

Yield strength

ABSTRACT

Introduction. The calculation of temperature during high-speed milling of aluminum alloys is of interest, since temperature can act as one of the main limiting factors in choosing rational milling modes. This is especially important when milling thin-walled products used in aircraft construction, since its high values can lead to local warping of the structure. It is not possible to control the temperature factor in production conditions, which makes it necessary to develop a mathematical model for calculating temperature. **The purpose of the work** is to develop a methodology for predicting the cutting temperature during high-speed milling of aluminum alloy workpieces for cutting conditions, in which it is not possible to use cutting fluid. **Methods.** This paper presents experimental studies of the cutting temperature during high-speed milling of aluminum alloy workpieces without the use of cutting fluid using non-contact temperature measurement methods. The results obtained were used to determine the coefficients substituted into formulas for calculating temperatures on the front and back surfaces of the cutting blade. **Results and discussions.** Based on the results of experimental tests and theoretical modeling, a temperature graph is drawn up. A comparison of experimental studies of milling of aluminum alloy D16T, with changing cutting conditions (the cutting speed changed) with theoretical data, gave a satisfactory result. The average relative error when comparing experimental data with theoretical one is 6.05%. Based on experimental data, it can be concluded that the comparison of experimental data for measuring cutting temperatures is in satisfactory agreement with the proposed method of theoretical calculation of temperatures. The advantage of this technique is that it allows, without time-consuming and costly experimental studies, theoretically calculate (forecast) the temperatures on the front and back surfaces of the cutting blade, as well as the cutting temperature, for those narrow milling conditions, where effective heat removal from the cutting zone is impossible. It can also be used for milling aluminum alloys, the mechanical and thermophysical properties of which differ.

For citation: Gubin D.S., Kisel' A.G. Features of calculating the cutting temperature during high-speed milling of aluminum alloys without the use of cutting fluid. *Obrabotka metallov (tehnologiya, oborudovanie, instrumenty) = Metal Working and Material Science*, 2024, vol. 26, no. 1, pp. 38–54. DOI: 10.17212/1994-6309-2024-26.1-38-54. (In Russian).

Introduction

The high-speed metal milling process is characterized by a high intensity of heat release. Determining the maximum temperature value and its distribution over the cutting surfaces of the tool is important, since it affects the choice of cutting modes, tool durability, and the quality of the machined surface of the part [1, 2, 3]. Thus, the maximum temperature values in determining the processing strategy act as one of the main limiting factors of cutting. The mechanism of heat generation during cutting is quite complex, however, three main factors can be distinguished: plastic deformation of the material, inhomogeneous shear and friction of the chips against the front surface of the tool, as well as friction of the back surface of the tool

* Corresponding author

Kisel' Anton G., Ph.D. (Engineering), Associate Professor

Kaliningrad State Technical University,

1 Sovetsky Prospekt,

236022, Kaliningrad, Russian Federation

Tel.: +7 999 458-08-25, e-mail: kisel1988@mail.ru

against the workpiece material being processed. The heat caused by these processes heats the chip material to a temperature of 350–450 °C [4, 5, 6, 7] (this temperature range is typical for milling aluminum alloys). The resulting heat spreads into the workpiece and the tool at a rate that largely depends on the physical characteristics of the material being processed [8, 9].

The heat distribution in the cutting area can be divided into two sections – the temperature on the front surface, depending on the feed, the geometry of the cutting blade (front angle, angle of inclination of the cutting edge, angle in plan, angle of elevation of the screw groove, etc.), and the temperature on the back surface, depending on the number of revolutions, the width of the chamfer in wearing process.

The calculation of the contact temperatures on the front and back surfaces of the tool, as well as the cutting temperature of the cutting blade for milling aluminum alloys is based on:

– changes in mechanical properties (ultimate strength, percentage of elongation) at increased test temperatures;

– taking into account the combined effect of processes such as deformation and strain rate on the change in the value of the yield stress;

– taking into account the thermal and physical characteristics of the material being processed (heat conduction and thermal diffusivity coefficients), as well as the density of the material.

The temperature calculations during high-speed milling of aluminum alloys are of interest because temperature is a limiting factor in choosing a processing strategy. For example, when milling a wafer profile inside a fuel tank for launch vehicles, it is not possible to use cutting fluid. The thickness of the outer wall of the fuel tank is 2–3 mm [7, 10, 11].

In this milling process, the temperature on the surfaces of the cutting blade acts as a limiting factor, since its high values can lead to local warping of the structure [12, 13, 14]. It is not possible to control the temperature factor at production field. Therefore, it is necessary to calculate rational milling modes in which the cutting temperature does not exceed acceptable values [9, 15].

In connection with the above, there is a necessity to develop a mathematical model for high-speed milling of aluminum alloys, which, as a first approximation, takes into account the combined effect of temperature, strain rate and strain magnitude on the change in the yield stress of the processed aluminum alloy. The resulting model will make it possible to calculate temperatures on various surfaces of the cutting tool, as well as the cutting temperature in high-speed milling conditions, for cases where it is not possible to use cutting fluid.

The purpose of this paper is to develop a methodology for calculating the cutting temperature during high-speed milling of aluminum alloy workpieces.

To achieve this purpose, it is necessary to solve the following tasks:

- 1) to create a defining equation for the specific work of deformation during cutting;
- 2) to solve the defining equation and find its positions of extremum, which are heat sources;
- 3) to derive theoretical dependencies that allow calculating the temperature in the cutting zone during high-speed milling of aluminum alloy workpieces;
- 4) to conduct experimental studies to determine the cutting temperature at the specified parameters;
- 5) to compare the theoretical and experimental data obtained and draw a conclusion about the accuracy of predicting the cutting temperature in a calculated way.

Methods

The defining equation for calculating temperature is the dependence of the change in the ultimate strength of the processed material on three constituent factors that arise during cutting (milling) – temperature, deformation and strain rate. Each of these factors will be considered separately and justified.

In conditions of small strain (for example, during tension or compression) and minor changes in temperature and strain rate, the change in yield stress can be described by the law of simple loading [16, 17]:

$$\sigma_T(\varepsilon) = \sigma_0 \left(\frac{\varepsilon}{\varepsilon_0} \right)^m, \quad (1)$$

where where ε_0 is the strain corresponding to the stress σ_0 ; ε is the current value of the strain; m is the coefficient of deformation hardening equal to $0.3T'$ (where T' is the homological temperature of the processed material).

However, equation (1) cannot be used to determine the yield stress for highly dynamic cutting processes (which include high-speed milling), since it does not take into account changes in deformation temperature and strain rate for changes in yield stress. In addition, the deformation temperature and the strain rate have a joint effect on the change in the yield stress, and are not free multipliers, as stated in a number of papers [18, 19].

The influence of temperature and strain rate in various equations for modeling changes in yield stress is taken into account by introducing appropriate multipliers. In particular, at present, the most popular *Johnson-Cook* plasticity model, which determines the behavior of a material during hardening, takes into account the influence of the strain rate on the change in yield stress using the dynamic coefficient $K\varepsilon$ [17, 20].

However, in the *Johnson-Cook* equation, the dynamic factor does not depend on temperature changes [21], while experimental data obtained by a number of scientists [16, 22, 23] confirm the combined effect of strain rate and temperature on the dynamic factor (figure 1).

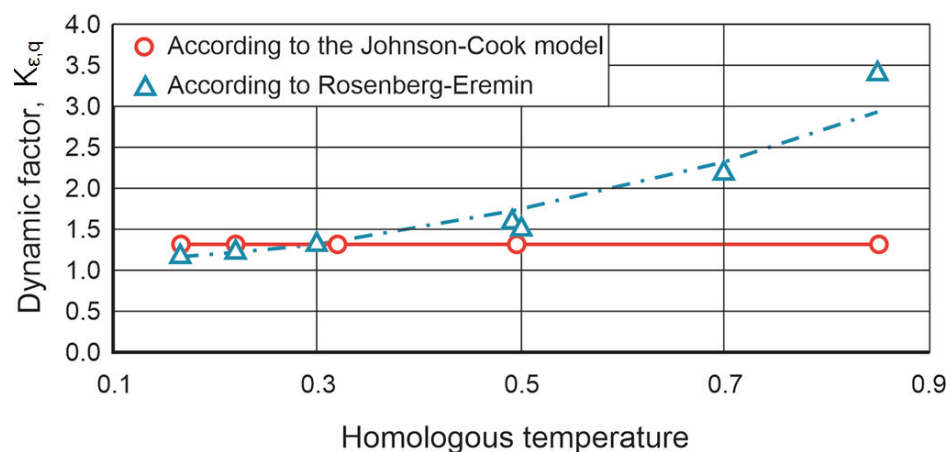


Fig. 1. Dependence of the Dynamic factor on the Homologous temperature [21, 24]

The diagram (figure 1) shows empirical results describing the influence of such factors as strain rate and homological temperature on the value of the dynamicity coefficient, as well as values approximated for the same conditions for the *Johnson-Cook* plasticity model [21]. In experiments, the strain rate varied by 1,000 and 2,000 times. And the change in homological temperature was achieved due to various processing materials (copper, steel, lead, aluminum).

A group of aluminum alloys *DI6T*, *AMg6*, *2024-T3* was selected for the research because it has similar physical properties and can be used for the manufacture of fuel tanks in the aircraft and rocket industry.

The calculations carried out in this research were performed on the basis of the dependences of the change in the actual ultimate strength on temperature during high-temperature tests of aluminum alloys (Table 1) [18, 19].

Based on Table 1, graphs of the change in ultimate strength versus test temperature were plotted (figure 2).

These graphs were approximated by an exponential curve with an accuracy of 0.9351 for the *DI6T* alloy and 0.9544 for the *AMg6M* alloy, which gives satisfactory results. Exponential extrapolation was chosen due to the fact that exponential equations are easier to integrate and differentiate than, for example, equations with polynomial dependence (although polynomial interpolation is a little more accurate), and linear approximation gives less accurate values for alloy *DI6T* and is 0.8971, and for alloy *AMg6M* practically does not differ from exponential and is 0.9318.

Table 1

**Strength and temperature characteristics obtained during monotonic tensile tests
of aluminum alloy specimens**

Material (aluminium alloy)	Test temperature t , (°C)	Ultimate strength σ_u , (MPa)	Ultimate elongation δ , (%)	Ultimate true strength S_u , (MPa)	Homologous temperature increment	Ratio of ultimate true strength at room temperature to ultimate true strength at test temperature
<i>D16T*</i>	20	460	19	523.6	0.31	1
	150	380	19	452.2	0.45	0.86
	200	330	11	366.3	0.5	0.7
	250	220	13	248.6	0.56	0.47
	300	150	13	169.5	0.61	0.32
<i>AMg6M*</i>	20	320	0.24	396.8	0.32	1
	100	300	0.3	390	0.4	0.98
	150	250	0.37	342.5	0.46	0.97
	200	190	0.43	271.7	0.51	0.68
	250	160	0.45	232	0.57	0.58
	300	130	0.48	192.4	0.62	0.48
	20	320	0.24	396.8	0.32	1
	100	300	0.3	390	0.4	0.98

* rolled semi-fabricated product (sheets)

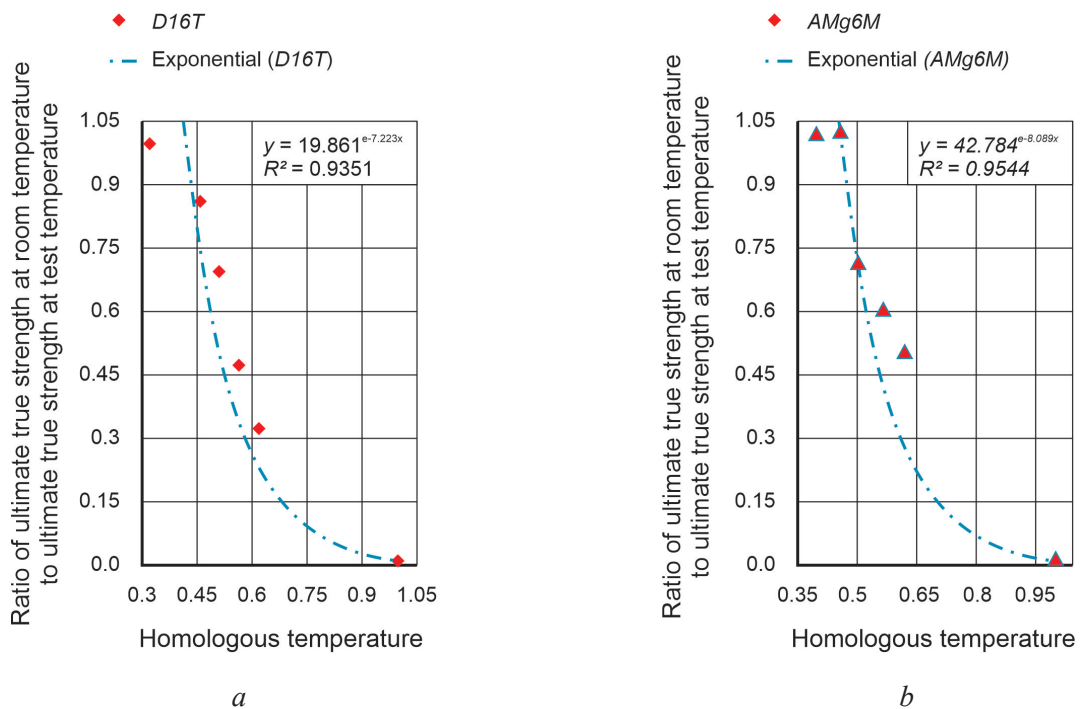


Fig. 2. Changes in the mechanical properties of aluminum alloys *D16T* (a) and *AMg6M* (b)

For these dependencies, an equation of the influence of temperature on the yield stress can be compiled:

$$\tau_p = S_{b20^\circ} \cdot e^{-h\Delta T'} \quad (2)$$

where S_{b20° is the value of the actual ultimate strength at room temperature; $\Delta T'$ is the increment of the homological temperature; h is the empirical coefficient of temperature softening.

Taking into account the experience of other researchers and based on experimental data (figure 1), it is possible to write the equation for the dynamic coefficient, taking into account temperature and strain rate, in the following form:

$$K_{\dot{\varepsilon}} = \left(\frac{\dot{\varepsilon}}{\dot{\varepsilon}_0} \right)^{k\Delta T'} \quad (3)$$

where $\dot{\varepsilon}$ is the current value of the strain rate; $\dot{\varepsilon}_0$ is the minimum value of the strain rate; k is an empirical constant.

From the above stated, it is possible to make a defining equation for the change in yield stress, taking into account the influence of deformation, strain rate and temperature:

$$\frac{\tau_p}{S_u} = A \left(\frac{\varepsilon}{\varepsilon_0} \right)^m \left(\frac{\dot{\varepsilon}}{\dot{\varepsilon}_0} \right)^{k\Delta T'} e^{-h\Delta T'} \quad (4)$$

$$\frac{\tau_p}{S_u} = A \varepsilon_p^m K_{\dot{\varepsilon}} e^{-h\Delta T'} \quad (5)$$

where ε_p^m is the multiplier responsible for the deformation hardening of the material; $K_{\dot{\varepsilon}}$ is the dynamic coefficient; $e^{-h\Delta T'}$ is the multiplier responsible for the temperature softening of the material; A is the deformation coefficient; S_u is the ultimate true strength.

However, in equation (5), deformation, strain rate and temperature act as three independent factors [21]. For example, a variation in the homological temperature can be achieved by heating the material being processed, and a modification of the deformation can be achieved by changing the geometry of the cutting blade (front angle). Therefore, using such a formula will lead to errors. In connection with this, it is necessary to move from the defining equation (5) to the specific work.

Specific work for the process of cutting materials in general and in particular for milling aluminum alloys is the most convenient parameter, since it combines the dependence of yield stress and the increment of homological temperature [19, 25]:

$$A_W = \int_0^{\varepsilon_u} \tau_p \varepsilon_p \quad (6)$$

where τ_p is the current value of the yield stress; ε_p is the current value of the deformation; ε_u is the final value of the deformation.

In the mathematical apparatus, it is most convenient to use differential equations to approximate calculations, and therefore it is necessary to replace the yield stress in equation (5) with the derivative of the specific work on deformation:

$$\frac{\tau_p}{S_u} = \frac{dA_W}{d\varepsilon_p} \quad (7)$$

To simplify calculations, we assume that heat transfer conditions close to adiabatic occur in the chip formation zone. Then, taking into account this approximation, the specific work of the deformation can be written as:

$$A_W = \Delta T' c_v, \quad (8)$$

where c_v is the specific thermal capacity of the processed material.

By virtue of formula (8), the part of equation (5), which is responsible for the temperature factor, is a function of the specific work of deformation. And the following equality is fair for it:

$$F(A_W) = e^{-hA_1 A_W}, \quad (9)$$

where $A_1 = \frac{S_b}{C_V T_{melt}}$ is a dimensionless group.

Now that all the parameters responsible for changing the yield stress during milling of aluminum alloys have been determined, it is possible to write the defining equation in differential form to determine the specific work of deformation:

$$\frac{dA_W}{d\varepsilon_p} = AK_{\varepsilon} \varepsilon_p^m e^{-hA_1 A_W}. \quad (10)$$

The dependence of specific work on deformation during milling aluminum alloys allows obtaining an analytical expression for constructing the flow curve of these alloys:

$$A_W = AK_{\varepsilon} \varepsilon_p^m e^{-hA_1 A_W} d\varepsilon_p. \quad (11)$$

But since aluminum alloys (in particular *DI6T*, *AMg6M*, *2024-T3*) are practically not strengthened during milling, due to the action of such a softening factor as temperature [19], then the construction of an analytical flow curve does not make sense. However, it makes sense to determine the maximum values of the yield stress, that is achieved during milling [16, 17, 20, 21].

The front surface during high-speed milling is characterized by homological temperatures above 0.5, and therefore, graphically (figure 1, according to *Rosenberg-Eremin*) the coefficient K_q equal to 1.8 was determined. And for the back surface (near the cutting edge) homological temperatures from 0.3 to 0.35 are characteristic; therefore, the dynamic coefficient K_{ε} equal to 1.25 was also determined graphically (figure 1, according to *Rosenberg-Eremin*).

After compiling a defining equation for modeling changes in the properties of the material being processed under high-speed milling conditions, one can proceed to calculating temperatures. However, in this work, the term “temperature” should be applied to the surface of the cutting blade (tooth) on which this temperature occurs. In this regard, it is necessary to distinguish between the temperature that occurs on different parts of the cutting blade, in particular on the front and back surfaces, as well as the temperature that results from these temperatures – the cutting temperature [26]. The cutting temperature is the result of the average temperatures occurring on the front and back surfaces of the cutting blade, related to the value of the coordinates on which these temperatures are distributed.

It should be noted that during milling, measuring the temperature on the front and back surfaces of the cutting blade is very difficult, since the cutting area is closed in front with chips, and behind with the material (workpiece) being processed. Therefore, all temperature measurements will be compared with the cutting temperature, that is, with the temperature measured by the thermal imager, in order to observe the temperature distribution on the surface under study.

To calculate the cutting temperature, a sufficiently large number of factors should be taken into account. It can be divided into factors that relate to the material being processed, factors that relate to the tool, and factors that are characteristic of the cutting process itself (turning, milling, drilling, etc.).

A necessary and obligatory condition for calculating the cutting temperature is the introduction of the mechanical and physical properties of the processed material into the model. These properties and characteristics for the group of aluminum alloys presented in Table 2 [18, 19]:

Mechanical and physical properties of aluminum alloys required for temperature calculations

Material grade	Ultimate strength σ_u , (MPa)	Ultimate elongation δ , (%)	Heat conductivity factor λ , (W/m·K)	Volumetric specific heat C_{Vp} , (MJ/m ³ ·K)	Temperature diffusivity coefficient ω , (m ² /s)	Density ρ , (kg/m ³)
D16T*	460	16	120	2.56	$4.95 \cdot 10^{-5}$	2,800
AMg6M*	320	24	122	2.43	$5.44 \cdot 10^{-5}$	2,640
2024-T3*	435	15	121	2.43	$5.68 \cdot 10^{-5}$	2,780

* Rolled sheets

In addition, to simulate the temperature calculation, it is necessary to take into account the geometry of the cutting tool (front angle γ , back angle α , cutting edge inclination λ , peripheral angle φ). It is equally important to determine the schematization of the milling process (terminal, cylindrical, end), and also take into account such parameters as the cutting depth e , the ratio of the milling width to the diameter of the cutter and the number of teeth working simultaneously.

For example, a changing in the front angle γ leads to a change in the inclination of the conditional shear plane, a change in the ratio of the contact length to the thickness of the cut layer, a change in the deformation, which ultimately affects the change in cutting powers [24].

Changing the inclination angle of the cutting edge (angle of elevation of the screw groove) and the angle in plan (peripheral angle) leads to a change in the thickness and width of the cut layer, which also affects the cutting powers:

$$b = \frac{t}{\sin \varphi \cdot \cos \lambda}; \quad (12)$$

$$a = S_z \sin \theta_m \cdot \cos \lambda, \quad (13)$$

where a and b are the thickness and width of the cut layer, accordingly; t is the milling depth; S_z is the feed to the tooth; θ_m is the angle of contact of the milling tooth with the processed material.

To improve the accuracy of calculations, such characteristics as the *Peclet* – Pe criterion, characterizing the speed of the heat source movement and the *Peclet* – K_{pe} coefficient, taking into account heat exchange with the environment, were added into the model [16, 17, 27]. Changes in the properties of the processed material depending on changes in the cutting temperature were also taken into account (figure 3–4).

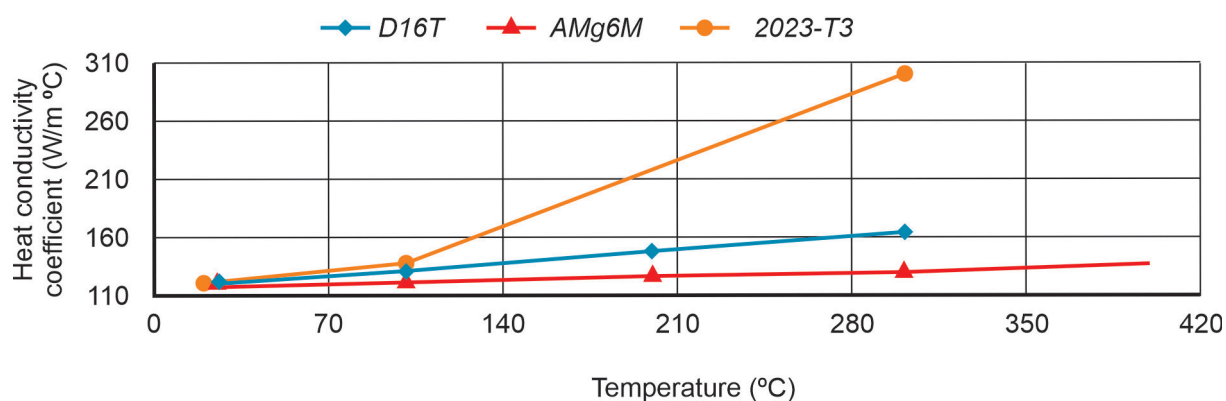


Fig. 3. Changes in the heat conductivity coefficient of the studied group of materials depending on temperature changes

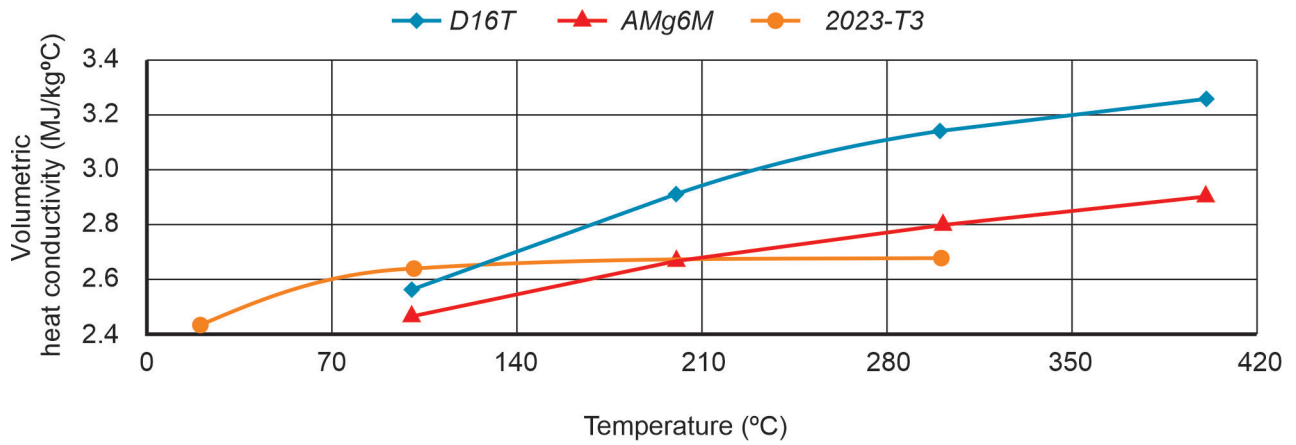


Fig. 4. Changes in Volumetric specific heat of the studied group of materials depending on temperature changes

To take into account for the heat transfer between the workpiece–environment–tool system, the milling process should be considered quasi-adiabatic. Therefore, the exponent in equation (11) can be written as:

$$\Delta T' = K_{Pe} \cdot A_W \cdot A_1; \quad (14)$$

$$A_1 = \frac{S_u}{C_V T_{melt}}. \quad (15)$$

Taking into account the equations (14, 15) it is possible to write the defining equation of specific work for a quasi-adiabatic process:

$$A_W = A \varepsilon_p^m K_\varepsilon \exp(-B_q A_1 A_W K_{Pe}) d\varepsilon. \quad (16)$$

Now it makes sense to determine the maximum yield stress values achievable with high-speed milling of aluminum alloys for specific deformation work. It can be determined after differentiating and integrating equation (16) of the specific work of deformation:

$$\tau_{q \max} = \frac{S_{u0} \cdot B \cdot A \cdot K_q \cdot \tilde{\varepsilon}_q^m}{m + 1}; \quad (17)$$

$$\tilde{\varepsilon}_{q \max} = \left(\frac{m(m+1)}{J \cdot B \cdot A \cdot A_1 \cdot K_q \cdot K_{Pe}} \right)^{\frac{1}{m+1}}. \quad (18)$$

Formulas (17) and (18) are common for both the front and back surfaces of the cutting blade. The difference lies in the different values of the dynamic coefficient due to the different values of homological temperatures on the contact surfaces of the tooth. For the front surface, the dynamic coefficient K_q is accepted as equal to 1.8, and for the back surface it is accepted as equal to 1.25.

Taking into account equations (7, 8), dependences (17, 18) can be considered to be heat sources on the front and rear surfaces of the cutting blade [20, 27]. The maximum values of contact temperatures on the front and back surfaces of the cutting blade were calculated numerically from these different heat sources for the back and front surfaces of the cutting blade in the *MS Excel* software environment.

Since the studied group of aluminum alloys obeys the general law of softening for this group (figure 2) and can be approximated by an exponential curve with a sufficiently high accuracy (above 0.93), any of these alloys can be selected to calculate the temperature. So, for example, the calculation performed for milling aluminum alloy *D16T*. The milling parameters were as follows: a carbide milling cutter with

a diameter of 10 mm with two teeth, the angle in plan $\varphi = 90^\circ$, the angle of inclination of the cutting edge $\lambda = 30^\circ$, the actual back angle $\alpha = 8^\circ$. The milling modes were as follows: $V = 471$ m/min; $S_m = 5,490$ mm/min; $S_z = 0.183$ mm/tooth; $n = 15,000$ rpm; $t = 0.5$ mm (fig. 5–6).

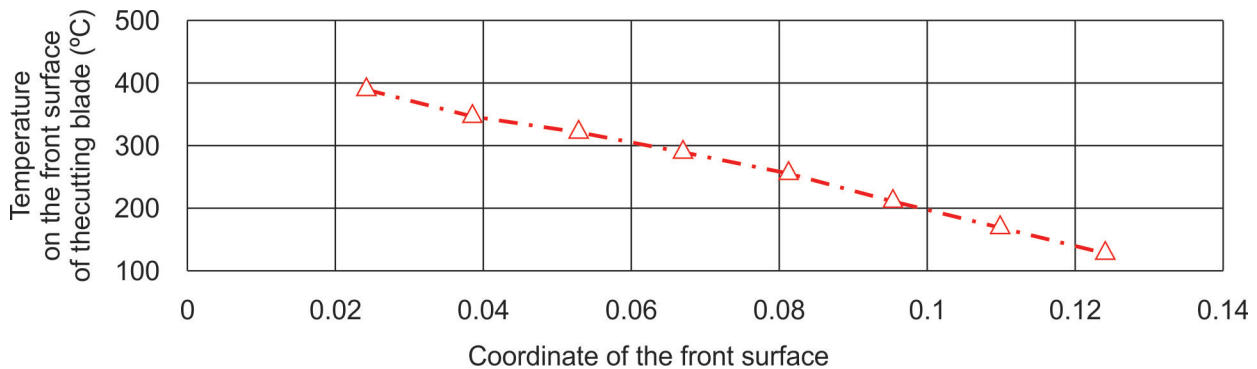


Fig. 5. Theoretical modeling of the temperature distribution on the front surface of the cutting blade

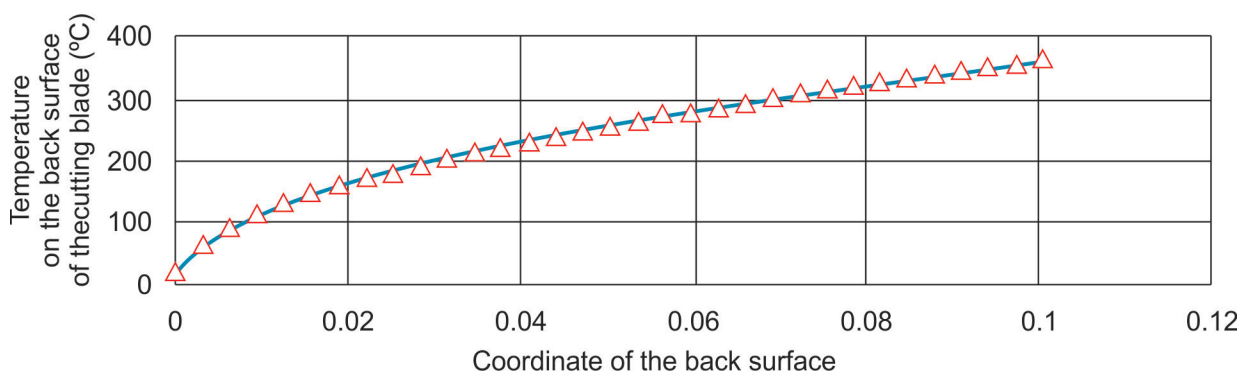


Fig. 6. Theoretical modeling of the temperature distribution on the front surface of the cutting blade

At the moment of cutting the cutter into the workpiece, since the pocket was being processed, it worked on both sides, therefore, passing and counter milling was implemented from different sides. On subsequent passes, counter milling was performed in order to eliminate machine backlashes and improve the quality of processing.

The cutting temperature was calculated based on the average values of the temperature on the front surface multiplied by the contact length of that face, and the temperature at the back surface multiplied by the width of the wear chamfer:

$$T_{cut} = \frac{T_{FrSur_{medium}} \cdot c + T_{BackSur_{medium}} \cdot h_{back}}{c + h_{back}} \quad (19)$$

This method of temperatures calculating allows clearly seeing the temperature distribution on the front and back surfaces of the cutting blade.

Results and discussion

A series of experiments on milling workpieces with a size of 250×40×120 mm made of aluminum alloy D16T was carried out to verify the theoretical calculation of temperatures. The mechanical characteristics and physical properties of this alloy are presented in Table 3.

An uncoated end mill of the *Hanita 4002* model with a diameter of 10 mm with a flat end face, with a number of tooth equal to 2 and a cutting edge inclination of 60° was used in the tests (figure 7).

All tests were carried out without the use of cutting fluid. The experimental factors were the cutting speed, that is, a one-factor experiment conducted with five levels of factor variation. To record the

Mechanical and physical properties of the processed alloy D16T

Material grade	Ultimate strength σ_u , (MPa)	Ultimate elongation δ , (%)	Heat conductivity factor λ , (W/m·K)	Volumetric specific heat C_p , (MJ/m ³ ·K)	Temperature diffusivity coefficient ω , (m ² /s)	Density ρ , (kg/m ³)
D16T	460	10	120	2.43	$5.44 \cdot 10^{-5}$	2,800

TYPE 4002



Fig. 7. Hanita 4002 carbide 2-tooth milling cutter

temperature during milling, a non-contact method was used, which allows continuous readings to be taken at a certain distance. The registration of measurements recorded using a *Fluke Ti400* thermal imager with a temperature field measurement error of 2 %. In the settings of the thermal imager, the radiation coefficient characteristic of aluminum alloys was selected, equal to 0.25.

All mechanical processing tests carried out on a multi-axis boring machine *2431SF10* with a *DRU* with an upgraded spindle, which allows reaching a rotation speed of 18,000 rpm. The experiments were carried out with fixed feed values per tooth and different values of cutting speed.

The experimental system “tool – workpiece – thermal imager” is shown in figure 8.

Figure 9 shows an example of non-contact temperature measurement for the following cutting modes: a) $n = 8,000$ rpm; $V = 251.2$ m/min; $S_z = 0.183$ mm/tooth; b) $n = 10,000$ rpm; $V = 314$ m/min; $S_z = 0.183$ mm/tooth.

Based on the results of the experimental data, a graph made of the temperature dependence on the change in the factor (in this case, the cutting speed) at all five levels of variation (figure 10).

To increase the accuracy of cutting temperature calculations, we also took into account the fact that the properties of the material being processed change with changes in the deformation temperature.

The test results can be summarized and presented in tabular form, where the average values of the experimental cutting temperature obtained from the results of three tests for each of the five levels of variation in cutting speed are calculated. The ratio errors in comparing the temperature values are also calculated (Table 4).

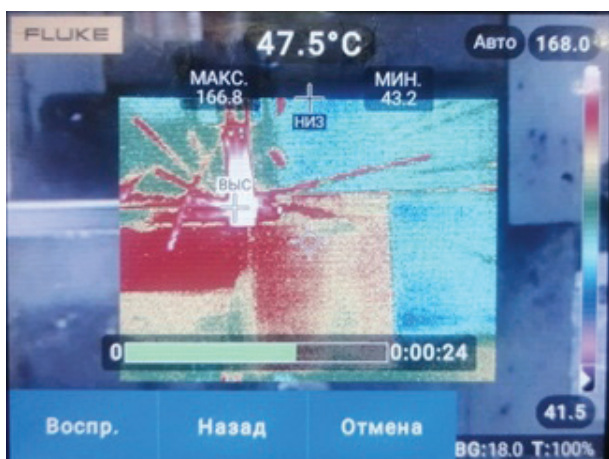
The average cutting temperature was compared with the average temperature of the contact surfaces of the cutting blade (eq. 19) and this result can be represented as a graph (figure 10):

Based on the results of experimental tests and theoretical modeling, a temperature graph is made (figure 11).

As a result of the work done, a mathematical model for calculating the temperature for high-speed milling of the studied group of aluminum alloys was developed. This model is based on reference data on high-temperature deformation of aluminum alloys, data on the mechanical and thermal and



Fig. 8. Experimental system for temperature measurement



a



b

Fig. 9. An example of temperature measurement for 8,000 rpm (a) and 10,000 rpm (b) with a Fluke Ti400 thermal imager

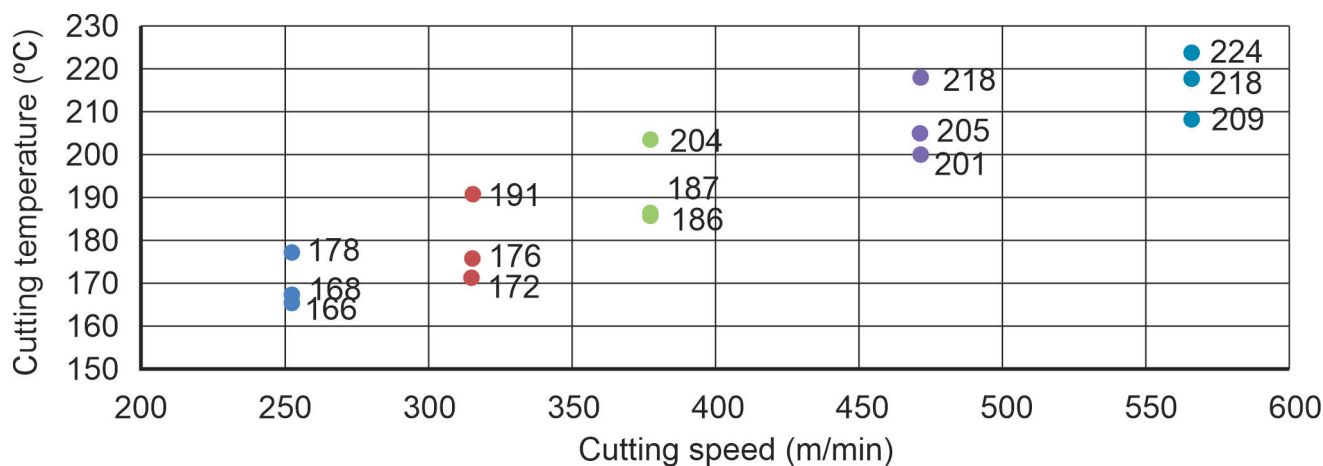


Fig. 10. Experimental values of the cutting temperature

physical properties of materials being processed, as well as experimental results on the study of the effect of deformation and strain rate on changes in the yield stress of materials during cutting. This model, as a first approximation, allows predicting the temperature values for a fairly wide range of milling parameters. In our case, the cutting speed varied from 251.2 to 562.2 m/min, and the rotation speed varied from 8,000 to 18,000 rpm.

The proposed solution for predicting the cutting temperature makes it possible at production field, without using time-consuming and expensive temperature measurement methods, theoretically calculate the temperature value using a computer and MS Excel software environment.

Conclusions

The evaluation of the results allowed us to draw the following conclusions:

1. Theoretical dependences are derived that allow calculating the temperature in the cutting zone during high-speed milling of aluminum alloy workpieces.
2. Experimental studies are carried out to determine the cutting temperature at the specified milling parameters.
3. Experimental data on measuring cutting temperatures are in satisfactory agreement with the proposed method of theoretical calculation of temperatures. The ratio error in comparing experimental data with theoretical data is 6.05 %.



Table 4

The results of experimental studies on the calculation of the cutting temperature when milling the *D16T* alloy and the corresponding theoretical calculations

Expt. No.	Speed (m/min)	$T_{\text{expt.}}$ (°C)	$T_{\text{expt.}}$ mean value (°C)	$T_{\text{calc.}}$ (°C)	Ratio error (%)
1	251.2	166	170.7	160	6.268307
	251.2	168			
	251.2	178			
2	314	191	179.7	170	5.397885
	314	172			
	314	176			
3	376.8	204	192.3	180	6.396256
	376.8	186			
	376.8	187			
4	471	218	208	196	5.769231
	471	205			
	471	201			
5	565.2	209	217	203	6.451613
	565.2	218			
	565.2	224			
mean value					6.056658

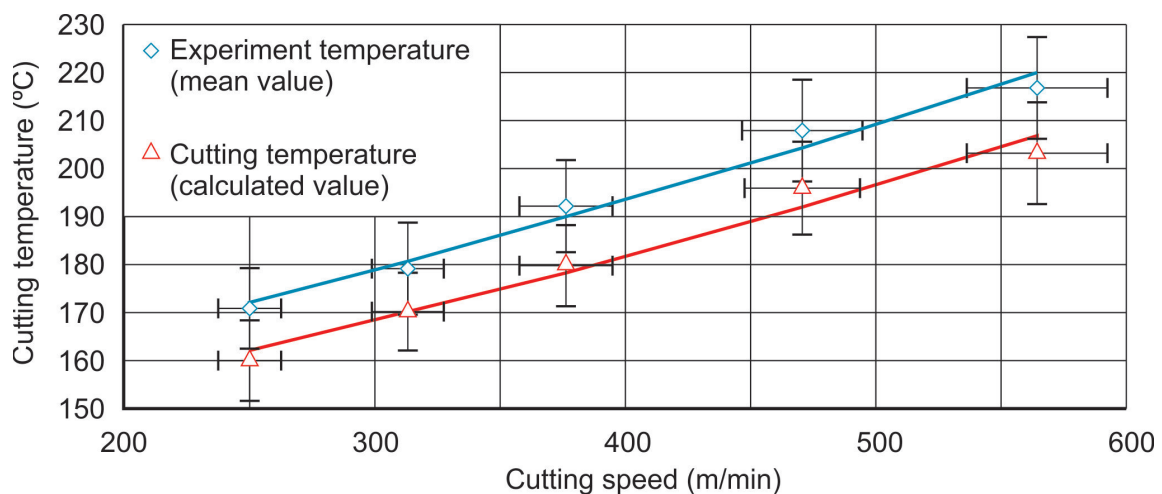


Fig. 11. Comparison of experimental and theoretical values of cutting temperature when milling aluminum alloy *D16T*

The results obtained confirm the correctness of the calculation formulas and that this technique allows, without time-consuming and costly experimental studies, theoretically calculate (forecast) the temperatures on the front and back surfaces of the cutting blade, as well as the cutting temperature, for those narrow milling conditions where effective heat removal from the cutting zone is impossible.



References

1. Wang S.J., Chen X., To S., Ouyang X.B., Liu Q., Liu J.W., Lee W.B. Effect of cutting parameters on heat generation in ultra-precision milling of aluminum alloy 6061. *International Journal of Advanced Manufacturing Technology*, 2015, vol. 80, pp. 1265–1275. DOI: 10.1007/s00170-015-7072-8.
2. Safiei W., Rahman M.M., Yusoff A.R., Arifin M.N., Tasnim W. Effects of SiO₂-Al₂O₃-ZrO₂ tri-hybrid nanofluids on surface roughness and cutting temperature in end milling process of aluminum alloy 6061-T6 using uncoated and coated cutting inserts with minimal quantity lubricant method. *Arabian Journal for Science and Engineering*, 2021, vol. 46, pp. 7699–7718. DOI: 10.1007/s13369-021-05533-7.
3. Meng X.X., Lin Y.X. Chip morphology and cutting temperature of ADC12 aluminum alloy during high-speed milling. *Rare Metals*, 2021, vol. 40, pp. 1915–1923. DOI: 10.1007/s12598-020-01486-2.
4. Santos M.C., Machado A.R., Sales W.F., Barrozo M.A.S., Ezugwu E.O. Machining of aluminum alloys: a review. *International Journal of Advanced Manufacturing Technology*, 2016, vol. 86, pp. 3067–3080. DOI: 10.1007/s00170-016-8431-9.
5. El-Eskandarany M.S., Aoki K., Sumiyama K., Suzuki K. Cyclic solid-state transformations during ball milling of aluminum zirconium powder and the effect of milling speed. *Metallurgical and Materials Transactions A*, 1999, vol. 30, pp. 1877–1880. DOI: 10.1007/s11661-999-0185-7.
6. Luo H., Wang Yq., Zhang P. Simulation and experimental study of 7A09 aluminum alloy milling under double liquid quenching. *Journal of Central South University*, 2020, vol. 27, pp. 372–380. DOI: 10.1007/s11771-020-4302-5.
7. Grubby S.V., Zaicev A.M. Obosnovanie uslovii frezerovaniya karmanov v korpusnykh detalyakh iz alyuminievykh splavov [The provement of the conditions of end mill operation in external panels of the aluminum alloys]. *Nauka i obrazovanie: nauchnoe izdanie MGTU im. N.E. Baumana = Science and Education: scientific periodical of the Bauman MSTU*, 2014, no. 5, pp. 12–30. DOI: 10.7463/0514.0709770.
8. Chatti S., Laperrière L., Reinhart G., Tolio T., eds. *CIRP encyclopedia of production engineering*. Berlin, Heidelberg, Springer, 2019. 1832 p. DOI: 10.1007/978-3-662-53120-4.
9. Il A., Chatelain J.F., Lalonde J.F., Balazinski M., Rimpault X. An experimental investigation of the influence of cutting parameters on workpiece internal temperature during Al2024-T3 milling. *International Journal of Advanced Manufacturing Technology*, 2018, vol. 97, pp. 413–426. DOI: 10.1007/s00170-018-1948-3.
10. Grubby S.V., Zaicev A.M. Issledovanie kontsevykh frez pri frezerovanii korpusnykh detalei iz alyuminievykh splavov [Research of end mills during milling of body parts made of aluminum alloys]. *Nauka i obrazovanie: nauchnoe izdanie MGTU im. N.E. Baumana = Science and Education: scientific periodical of the Bauman MSTU*, 2013, no. 12, pp. 31–54. DOI: 10.7463/1213.0634375.
11. Ming W., Yu W., Qiu K., An Q., Chen M. Modelling of the temperature distribution based on equivalent heat transfer theory and anisotropic characteristics of honeycomb core during milling of aluminum honeycomb core. *International Journal of Advanced Manufacturing Technology*, 2021, vol. 115, pp. 2097–2110. DOI: 10.1007/s00170-021-06943-5.
12. Duan Z., Li C., Ding W., Zhang Y., Yang M., Gao T., Cao H., Xu X., Wang D., Mao C., Li H.N., Kumar G.M., Said Z., Debnath S., Jamil M., Ali H.M. Milling force model for aviation aluminum alloy: academic insight and perspective analysis. *Chinese Journal of Mechanical Engineering*, 2021, vol. 34, p. 18. DOI: 10.1186/s10033-021-00536-9.
13. Bugdayci B., Lazoglu I. Temperature and wear analysis in milling of aerospace grade aluminum alloy Al-7050. *Production Engineering*, 2015, vol. 9, pp. 487–494. DOI: 10.1007/s11740-015-0623-x.
14. Kugultinov S.D., Shchenyatskii A.V., Zhilyaev A.S. Chislennyi analiz vliyaniya uslovii mekhanicheskoi obrabotki na napryazhenno-deformirovannoe sostoyanie krupnogabaritnykh tonkostennykh detalei slozhnoi formy [Numerical analysis of influence of mechanical processing conditions on stress-deformed state of large-size thin-wall complex parts]. *Intellektual'nye sistemy v proizvodstve = Intelligent Systems in Manufacturing*, 2018, vol. 16 (3), pp. 17–21. DOI: 10.22213/2410-9304-2018-3-17-21.
15. Trusov V.N., Zakonov O.I., Shikin V.V. Issledovanie parametrov protsessa frezerovaniya alyuminievogo splava D16T [Research on milling parameters for the D16T aluminium alloy]. *Vestnik Samarskogo gosudarstvennogo tekhnicheskogo universiteta. Seriya: Tekhnicheskie nauki = Vestnik of Samara State Technical University. Technical Sciences Series*, 2012, no. 3 (35), pp. 155–162. Available at: https://elibrary.ru/download/elibrary_18955077_35295693.pdf (accessed 09.02.2024).
16. Kushner V.S., Storchak M.G., Burgonova O.Yu., Gubin D.S. Razrabotka matematicheskoi modeli krivoi techeniya splavov pri adiabaticheskikh usloviyakh deformirovaniya [Mathematical modeling of the alloy flow curve in adiabatic conditions of deformation]. *Zavodskaya laboratoriya. Diagnostika materialov = Industrial*



laboratory. *Diagnostics of materials*, 2017, vol. 83 (5), pp. 45–49. Available at: https://elibrary.ru/download/elibrary_29197671_73184792.pdf (accessed 09.02.2024).

17. Burgonova O.Yu., Kushner V.S. *Povyshenie effektivnosti obrabotki konstruktivnykh materialov frezerovaniem* [Improving the efficiency of processing structural materials by milling]. Omsk, Omsk State Technical University Publ., 2013. 140 p. ISBN 978-5-8149-1640-2.

18. Gabrian International (H.K.) Ltd. Available at: <https://www.gabrian.com/2024-aluminum-properties/> (accessed 09.02.2024).

19. Grigor'ev I.S., Meilikhov E.Z., eds. *Fizicheskie velichiny: spravochnik* [Physical quantities: reference]. Moscow, Energoatomizdat Publ., 1991. 1232 p. ISBN 5-283-04013-5.

20. Kushner V., Storchak M. Determining mechanical characteristics of material resistance to deformation in machining. *Production Engineering*, 2014, vol. 8 (5), pp. 679–688. DOI: 10.1007/s11740-014-0573-8.

21. Huang X., Xu J., Chen M., Ren F. Finite element modeling of high-speed milling 7050-T7451 alloys. *Procedia Manufacturing*, 2020, vol. 43, pp. 471–478. DOI: 10.1016/j.promfg.2020.02.186.

22. Vorob'ev A.A., Krutko A.A., Sedykh D.A. Razrabotka modeli dlya otsenki napryazhenno-deformirovannogo sostoyaniya tverdosplavnogo instrumenta pri vosstanovitel'noi obrabotke zhelezodorozhnykh koles [Investigation of the stressed state of a carbide tool during turning of railway wheels]. *Naukoemkie tekhnologii v mashinostroenii = Science Intensive Technologies in Mechanical Engineering*, 2022, no. 12 (138), pp. 9–15. DOI: 10.30987/2223-4608-2022-12-9-15.

23. Zorev N.N., ed. *Razvitie nauki o rezanii metallov* [Development of metal cutting science]. Moscow, Mashinostroyeniye Publ., 1967. 415 p.

24. Rozenberg A.M., Eremin A.N. *Elementy teorii protsessa rezaniya metallov* [Elements of the theory of the metal cutting process]. Moscow, Mashgiz Publ., 1956. 318 p.

25. Gubkin S.I. *Plasticheskaya deformatsiya metallov*. T. 3. *Teoriya plasticheskoi obrabotki metallov* [Plastic deformation of metals. Vol. 3. Theory of plastic processing of metals]. Moscow, Metallurgizdat Publ., 1961. 306 p.

26. Zhiliaev A.S., Kugultinov S.D. Matematicheskoe modelirovanie teplovykh protsessov pri frezerovanii slozhnoprofil'nykh detalei iz alyuminievykh splavov [Mathematical simulation of thermal processes when milling aluminum alloy formed parts]. *Vestnik Kontserna VKO «Almaz – Antei»*, 2019, no. 2 (29), pp. 65–70. (In Russian). Available at: https://elibrary.ru/download/elibrary_41273368_35941140.pdf (accessed 09.02.2024).

27. Vereshchaka A.S., Kushner V.S. *Rezanie materialov* [Cutting materials]. Moscow, Vysshaya shkola Publ., 2009. 535 p.

Conflicts of Interest

The authors declare no conflict of interest.

© 2024 The Authors. Published by Novosibirsk State Technical University. This is an open access article under the CC BY license (<http://creativecommons.org/licenses/by/4.0>).